Article ID: 1006-8775(2020) 03-0286-14

Quality Assessment of FY−4A Lightning Data in Inland China

LIU Rui-xia (刘瑞霞) [1], LU Qi-feng (陆其峰) [1], CHEN Min (陈 敏) [2], ZHANG Yong (张 勇) [3], HUI Wen (惠 雯) [1], LI Xiao-qing (李小青) [1]

(1. Key Laboratory of Radiometric Calibration and Validation for Environmental Satellite, National Satellite Meteorological Center, China Meteorological Administration, Beijing 100081 China;
2. Institute of Urban Meteorology, China Meteorological Administration, Beijing 100089 China;
3. Meteorological Observation Center, China Meteorological Administration, Beijing 100081 China)

Abstract: The Lightning Mapping Imager (LMI) equipped on the FY-4A (FengYun-4A) geostationary satellite achieves lightning positioning through optical imaging and has the advantages of high temporal resolution, high stability, and continuous observation. In this study, FY-4A LMI lightning event, group and flash data from April to August 2018 are selected, and their quality are assessed through qualitative and quantitative comparison with the ground-based Advanced Time of Arrival and Direction system (ADTD) lightning observation network data and the American International Space Station (ISS) lightning imaging sensor (LIS) data. The results show that the spatial distributions of FY-4A lightning are consistent with those of the ground-based ADTD and ISS LIS. The temporal variation in FY-4A lightning group frequency is consistent with that of ADTD stroke, which reflects that FY-4A LMI can capture the lightning occurrence in inland China. Quantitative statistics show that the consistency rate of FY-4A LMI and ISS LIS events is relatively high but their consistency rate is lower in terms of lightning group and flash data. Compared with the lightning observations by the ISS LIS and the ground-based ADTD, FY-4A LMI reports fewer lightning events in the Tibetan Plateau. The application of Tibetan Plateau lightning data requires further processing and consideration.

Key words: FY-4A lightning data; quality assessment; inland China; ADTD; ISS LIS

CLC number: P412.27 **Document code:** A

https://doi.org/10.46267/j.1006-8775.2020.026

1 INTRODUCTION

Lightning refers to ultra-long-distance intense electrostatic discharge that occurs in the atmosphere, usually accompanied by strong convective weather processes. Lightning significantly affects fields such as weather analysis, aviation support, and military meteorology. Lightning disasters considered one of the ten most severe natural disasters by the United Nations. Accurate detection of lightning can improve the basis for disaster monitoring and prediction to reduce the loss of human lives and property. It has been gradually recognized that lightning plays very important roles in maintaining the circuit balance between the Earth and the ionosphere and in the formation of NO_x [1,2]. In addition, lightning plays an indicative role in climate change. Toumi et al. [3] proposed a positive feedback mechanism for tropospheric ozone, lightning, and climate change. In a warm climate, frequent lightning activities lead to an increase in the tropospheric ozone [3]. Williams et al. [4] found that lightning frequency can increase by up to 30% in response to a surface temperature increase of 1 ℃. The distribution and frequency of lightning are closely related to the El Niño-Southern Oscillation (ENSO) phenomenon [6, 7]. Lightning can convey information about many atmospheric processes, and hence, studies of lightning can promote the interpretation of phenomena in and make significant contributions to Earth system sciences, including weather, climate, atmospheric chemistry, and lightning physics [8−14].

Satellite lightning observation is characterized by a large detection range and observation height and is not subject to ground conditions, thereby enabling the intuitive and dynamic acquisition of lightning formation and development information from above [15]. The launch of the optical transient detector (OTD) in 1995 ushered in a new era of space-based lightning detection, which provided lightning frequency and distribution data covering almost the entire globe. In November 1997, the lightning imaging sensor (LIS), as part of the Tropical Rainfall Measuring Mission (TRMM), joined the on-orbit OTD, and the observational data have been widely used since then [16]. The LIS instrument was similar to the OTD except for its higher sensitivity. The inclination angle of the LIS relative to the equator was 35°, the observation area was between 35° S and 35° N, one full coverage of the globe required 49 days, and the TRMM/

Received 2019-08-28; **Revised** 2020-05-15; **Accepted** 2020-08-15

Funding: National Key R&D Program of China (2018YFC1506603); The Second Tibetan Plateau Scientific Expedition and Research (STEP) Program(2019QZKK0105)

Biography: LIU Rui-xia, Ph. D., Professor, primarily undertaking research on application of satellite data.

Corresponding author: LU Qi-feng, e-mail: luqf@cma.gov.cn

LIS was operated for 17 years [17]. The LIS and OTD provided the first real observations of lightning frequency, distribution, activity, and variations covering almost the entire globe. The LIS and OTD significantly advanced early stage observations of lightning [18]. In 2017, the International Space Station (ISS) LIS was launched. The ISS LIS integrates the advantages of the ISS platform (such as high inclination, real-time data, and colocated payloads), which extends the scientific mission of TRMM/LIS and OTD [8]. However, the low orbit of ISS LIS limits the temporal frequency of the data obtained.

Because both OTD and LIS are mounted on low-orbit satellites, their detection time at any point on the planet is extremely limited. The OTD requires 55 days to complete a full scan of the Earth, while the LIS needs 49 days. To a large extent, the detection time depends on the distance of the satellite from the Earth and the orientation of the detector. The detection time at high latitudes is 2−4 times longer than that near the equator [18], which significantly limits the comprehensive and real-time monitoring, tracking, and early warning of lightning activity in a fixed area. The first satellite of China's FengYun-4 satellite series (FY-4A) was successfully launched in December 2016. The Lightning Mapping Imager (LMI) on FY-4A is the first optical payload of geostationary lightning detection developed in China [19] and is one of the three optical payloads of geostationary lightning detection, with the other two developed by the United States and Europe during the same period. Geostationary lightning optical detection aims to achieving continuous and real-time detection of lightning in a fixed area, which is the most effective means of lightning detection[19] and is very useful for early predictions of storms and severe weather events [20~22]. With the exception of the fact that its field of view covers China and surrounding areas, other indicators of the FY-4A LMI are generally consistent with those of the European Meteosat Third Generation (MTG) Lightning Imager (LI) and the United States Geostationary Operational Environmental Satellites-R (GOES-R) Geostationary Lightning Mapper (GLM) [23,24]. GOES-R was launched in November 2016, and the MTG satellite is scheduled to be launched in 2020. The lightning data obtained by geostationary meteorological satellites have a very important value and potential for applications in fields such as weather analysis, aviation support, and military meteorology.

Therefore, in this study, China's FY-4A LMI data are assessed through comparison with satellite and ground-based lightning observations to provide support for the further effective application of these data.

2 DATA AND PROCESSING

2.1 *FY-4A lightning data*

The FY-4A LMI uses a charge-coupled device (CCD) plane array imaging detector with 400 (north-south) × 600 (east-west) pixels. The spatial resolution is 7.8 km at nadir [25], and the imaging rate is 500 frames s^{-1}. To realize the lightning detection of FY-4A LMI, spatial filtering, temporal filtering, spectral filtering, background dimming and other technologies are used to improve the signal-to-noise ratio of lightning signals. Furthermore, the lightning imager products are obtained by calibration and navigation processing, lightning false signal filtering and clustering analysis. The location accuracy of LMI can reach 1 pixel [19].

FY-4A LMI products include lightning event data as well as events clustering-formed group and flash data. Event data are the most basic unit of a lightning signal obtained by the FY-4A LMI. The LMI real-time event processor determines events by comparing the radiation after background dimming with a threshold and then extracts the pixels that exceed the threshold. On this basis, lightning products of different group and flash levels are generated through a cluster calculation process. The "group" is composed of "events" of the adjacent CCD plane array in the same frame, while "flash" is composed of "groups" with a time interval of no greater than 330 ms and a space distance of no more than 16.5 km [26].

An event is the basic data unit of lightning, and many advanced users can process group, flash and other data on the basis of event data. In lightning data assimilation and other fields, users also use event data more often, so in this study, the event, group and flash data observed by FY-4A LMI are selected to evaluate data precision and provide reference for data users.

The FY-4A LMI observes the Northern Hemisphere annually from mid-March to mid-September. The observation range is shown in Fig. 1, covering most of the land and sea areas of China and neighboring regions. For the rest of the year, FY-4A LMI turns around to observe the Southern Hemisphere, covering western and central Australia and neighboring waters. In this study, FY-4A lightning data in the inland areas of China within the period from April to August 2018 are evaluated.

2.2 *Ground-based ADTD lightning positioning data*

The ADTD lightning detection network data of the China Meteorological Administration (CMA) are selected for comparison with FY-4A LMI lightning data. As seen from the distribution figure of China's ADTD lightning observation stations (Fig. 2), more than 419 lightning stations are distributed in China. These ADTD stations are densely and relatively uniformly distributed in east China and are sparsely distributed in west China, especially in the Tibetan Plateau, due to its special geography and complex topography.

The ADTD mainly detects ground lightning. According to the detection mechanism, the ADTD determines the current parameters of lightning sources by simultaneously measuring the electromagnetic field of lightning return stroke radiation from several substations. The ADTD uses a combination of Magnetic

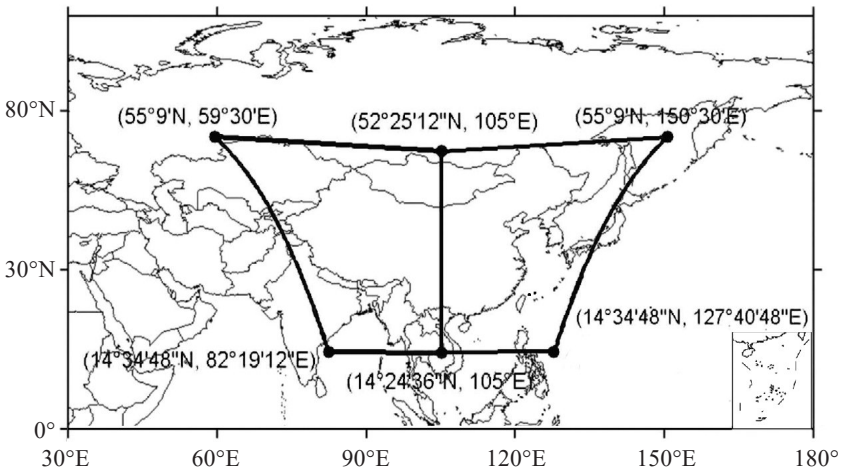

Figure 1. Observational area of the FY-4A LMI for China.

Direction-Finder and Time-of-Arrival methods to locate lightning. The detection range of substation is approximately 150 km [27, 28], and the time accuracy reaches 0.1us. According to Xia et al. [28], from manufacturer's report, the ADTD lightning detection network in central and east China has a detection efficiency of 90% and a location accuracy of approximately 500 m within a radius of 150 km, but in fact, the location error of the ADTD lightning data may reach 2 km. Meng et al. [29] also described that the detection efficiency of ADTD is 80% to 90%, and the error is generally several hundred meters to several kilometers. The operational network provides reports on the time of the returning stroke and its location (latitude and longitude), polarity, and intensity, etc. In this paper, we use the ADTD stroke data from April to August 2018 for comparison.

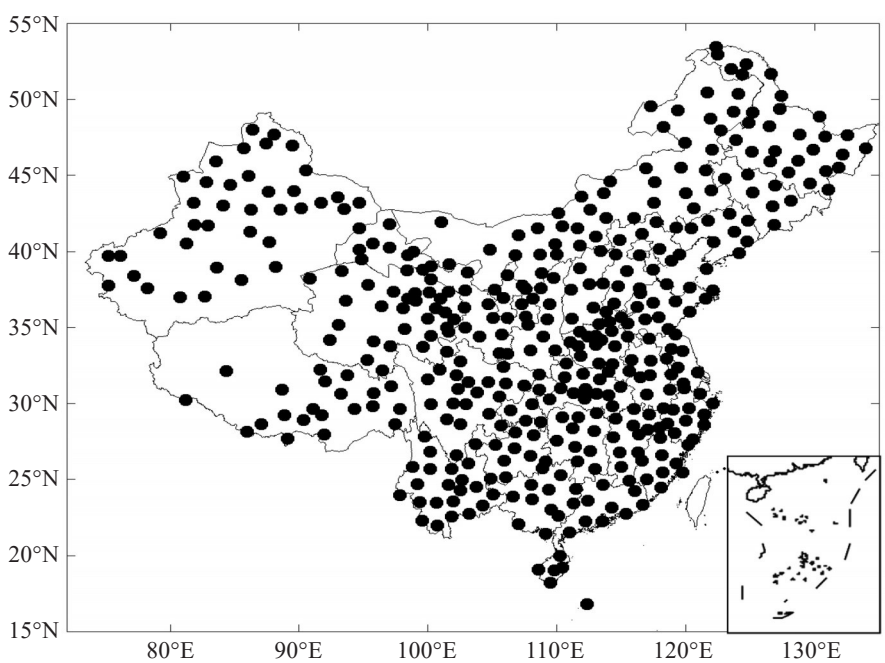

Figure 2. Ground-based ADTD lightning detection network in China.

2.3 *ISS LIS lightning data*

The LIS was mounted on the ISS in February 2017 and was fully integrated into the space station as part of the US Department of Defense Space Test Program-Houston 5 (STP-H5). It extends the LIS time-series observations from the TRMM. Compared with the TRMM LIS, the ISS LIS has a high-inclination orbit and can detect a larger geographic range. The latitude range of detection is +/− 54°, and the longitude range is +/− 180°. The resolution is 4 km at nadir, and the temporal resolution is less than 1 min. The ISS LIS measures lightning in the daytime and nighttime and covers almost the entire globe. The ISS LIS provides real-time (cloud and ground) lightning data over land and sea [30]. The detection efficiency of the ISS LIS event is approximately 90% with a location accuracy of 1

pixel [31,32]. ISS LIS data includes lightning event, group and flash. For comparison with the FY-4A LMI observations in inland China, the ISS LIS event, group, and flash data from April to August 2018 are used.

2.4 *Data processing*

FY-4A LMI and ISS LIS record the longitude and latitude positional information of each lightning event, group and flash, and ADTD records the position of return stroke. In this study, we first compare the spatiotemporal distribution of LMI, LIS and ADTD lightning. Therefore, it is necessary to convert the location information into lightning frequency for comparison. Inland China is divided into 0.5 °× 0.5 ° longitude and latitude grids, and the daily average lightning frequency in each grid is calculated to compare the spatial distribution and time variation trend.

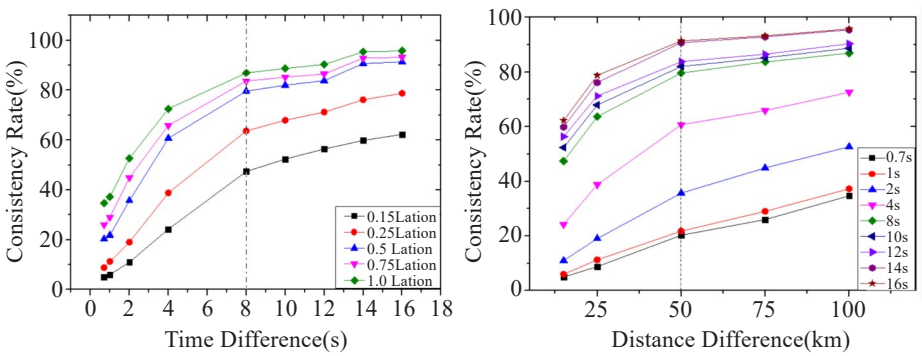

Figure 3. Relationship between the consistency ratio and time threshold and between the consistency ratio and space threshold for FY4 LMI and ISS LIS Lightning event data. The vertical black dotted line is the chosen time and space threshold.

For the quantitative comparison, the ISS LIS data are used as a criterion, and lightning data acquired by the ISS LIS and the FY-4A LMI during the same period are compared in this study. We establish a matching time/ space window, with lightning reported by both data types defined as a matched sample.

Through the sensitivity test, the threshold of time and space matching window is established to evaluate the consistency of two kinds of lightning observational data [33~35]. In this paper, the consistency ratio (CR) of FY4 LMI and ISS LIS lightning matching is defined as the proportion of FY4A LMI that can coincide with at least one ISS LIS observation in a specific study area to the total number of ISS LIS in that study area. As shown in Formula (1):

$$CR=N_{mat}/N_{LIS} \quad (1)$$

where N_{mat} is the number of LIS events that coincide with LMI events, and N_{LIS} is the total number of LIS events.CR value of 100% means that each ISS LIS in the study interval has at least one matching FY4 LMI; CR value of 0 means that there is no matching LIS and LMI observation in the study interval. We gradually adjust the space-time matching window size, and calculate the CR value of LIS and LMI event data under different time and space dimensions. The variation of CR value is shown in Fig. 3a and Fig. 3b respectively if the time interval is from 0.7s to 16s and the difference of longitude and latitude is from 0.15° to 1.0° between the two lightning data. CR value increases with the increase of the allowed time difference and the increase of the allowed space longitude and latitude difference. Select the time when the curve starts to flatten(8.0s) and the location point of the longitude and latitude (0.5° latitude and longitude) as the time-space threshold of the two lightning observational data matching. From here on, with the increase of the allowed time-space difference, the CR value will not increase significantly.

The matching method of group and flash is the same as that of event. The time/ space coincidence window for LIS and LMI events is set to be 8.0 s/0.5° too (Fig. 4 and Fig. 5).

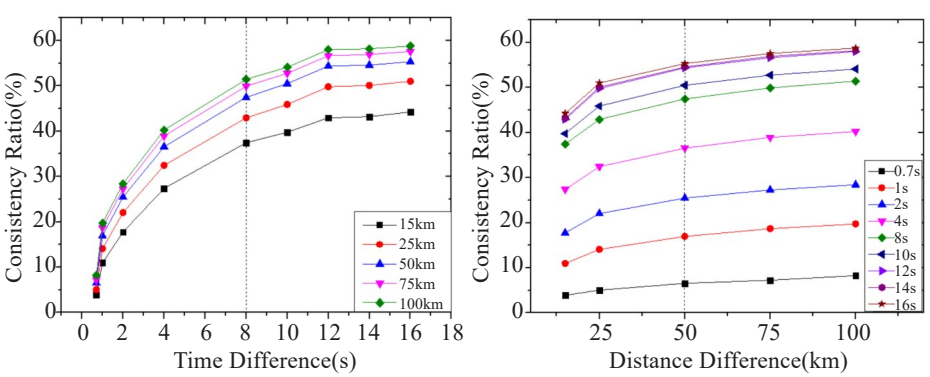

Figure 4. Relationship between the CR and time threshold and between the CR and space threshold for FY4 LMI and ISS LIS Lightning group data. The vertical black dotted line is the chosen time and space threshold.

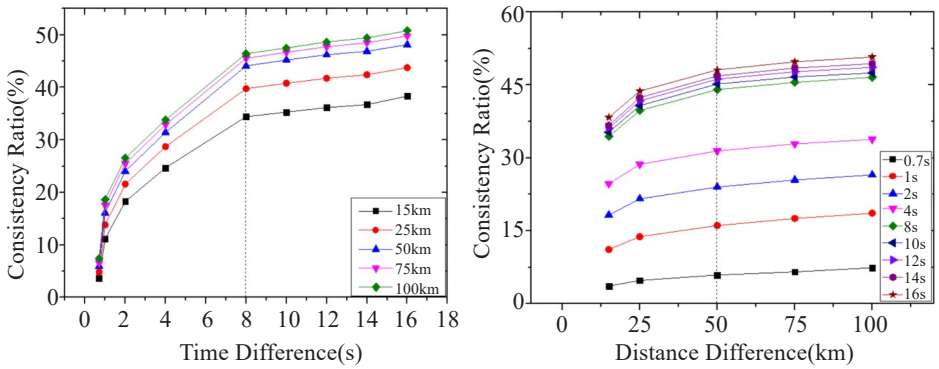

Figure 5. Relationship between the CR and time threshold and between the CR and space threshold for FY4 LMI and ISS LIS Lightning flash data. The vertical black dotted line is the chosen time and space threshold.

3 QUALITY ANALYSIS OF CHINA'S FY-4A LMI LIGHTNING DATA

3.1 *Comparison of the spatial distribution of lightning groups*

The spatial distribution of FY-4A LMI, ADTD and ISS LIS lightning are compared. Fig. 6 shows the spatial distribution of the daily mean occurrence frequency from the FY-4A LMI lightning group (Fig. 6a~6e), ADTD stroke (Fig. 6f~6j) and ISS LIS lightning group (Fig. 6k~6o) in inland China for each month from April to August 2018.

In April 2018, the high-value area of lightning group is mainly distributed in east and south China. Observations of FY-4A LMI, ADTD and ISS LIS all show lightning high-value zones located along the southern margin of Yunnan, Guizhou, Hunan, Jiangxi, Hubei, and Zhejiang (shown by the red line in Fig. 6a, 6f, 6m). The mean lightning group frequency in Hunan exceeds 700 times a day. Both spatial distribution pattern and value of ADTD stroke data in this high-value zone are very consistent with those of FY-4A LMI (Fig. 6f). The distribution pattern of the ISS LIS group is the same as that of FY-4A LMI, but the value magnitude of the former is much less than that of the latter, partly because of the ISS LIS carrying the polar orbiting satellite and only being capable of fixating on and observing a particular location for approximately 90 s. In addition, LMI and LIS have observed lightning in southern Gansu, southeast Tibet Plateau, Liaoning and Jilin, but ADTD has not. Therefore, the group spatial distribution of FY-4A LMI and ISS LIS is more consistent than that of ADTD, and this difference may be related to observation methods and the respective differences between the space-based and ground-based observation systems.

In May, the high-value areas of lightning occurrence are mainly distributed in south China, central China, east China and the southeast corner of the lower reaches of the plateau, among which south China has the highest frequency of lightning occurrence. FY-4A LMI, ADTD and ISS LIS all show the same distribution characteristics (Fig. 6b, 6g, and 6l). However, the lightning stroke number of ADTD in south China is significantly higher than that of FY-4A LMI lightning group. It is possible that the clustering analysis method of transforming a lightning event into a group introduces error. A small amount of lightning is observed in ISS LIS and FY-4A LMI in western Beijing and the northwest corner of Jilin Province, but not in ADTD.

From June to July, in addition to the high-value areas of lightning in south China, central China, east China and the southwest of the lower plateau, there is more lightning in northeast China due to the influence of the monsoon and northward extension of the rain belt of China. The distribution of FY-4A LMI, ADTD and ISS LIS for these lightning high-value areas is also consistent. However, the groups observed by FY-4A LMI in general are less than that observed by ADTD stroke (Fig. 6c, 6h, 6m, 6d, 6i, and 6n). In northeast China, the lightning group frequency of ISS LIS is higher than that of LMI and ADTD. In July, the frequency of the lightning group is also higher in north China and central Inner Mongolia, and the distribution of lightning in this region is consistent with the three kinds of data. A small amount of lightning is observed in FY-4 LMI and ISS LIS in the northern plateau and the southern edge of Xinjiang in July (Fig. 6d and 6n), but there is no lightning in this area in the ADTD distribution figure (Fig. 6i), which may be related to the dispersion of ground observation stations.

In August 2018, as shown in Fig. 6e, 6j, and 6o, an area of high lightning occurrence appeared in the eastern margin of Yunnan and Sichuan, while lightning occurrence in south China was still high (red circle). In addition, there was also a high lightning occurrence in Hebei Province (yellow circle). Comparison of the FY-4A LMI, ADTD and ISS LIS lightning group spatial distributions shows that the three datasets are consistent with regard to these two areas of high lightning occurrence. ISS LIS also detects lightning in northeast China, while FY-4A LMI and ADTD show low lightning value areas in the northeast. It is possible that ISS LIS overestimates lightning in the northeast. A small amount

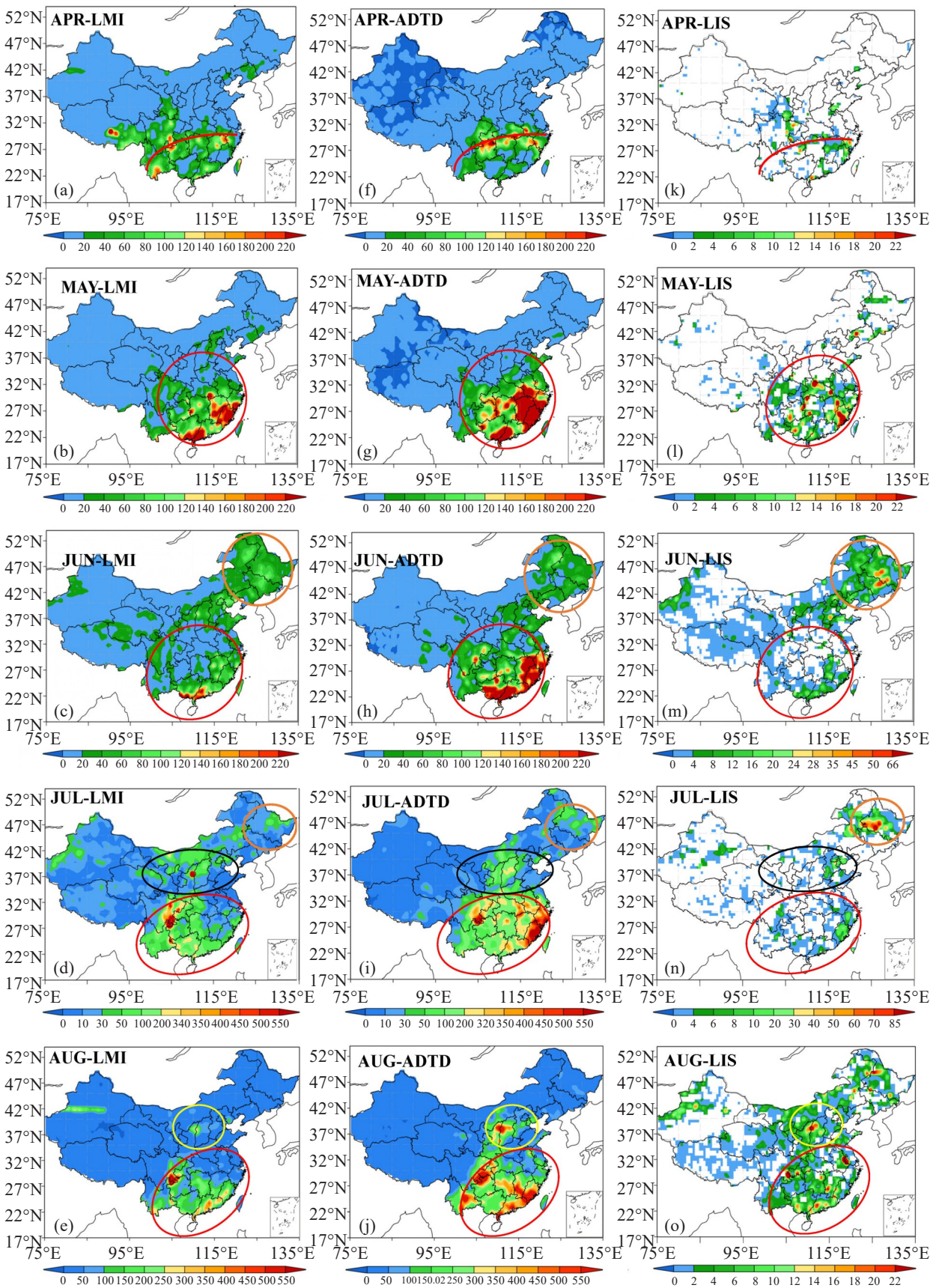

Figure 6. Spatial distribution of daily mean lightning in inland China in 2018. (a)-(e) are the daily mean lightning spatial distributions of FY-4A from April to August; (f)-(j) are the daily mean lightning spatial distributions of the ground-based ADTD lightning observation network from April to August; (k)-(o) are the daily lightning spatial distributions of the ISS LIS from April to August.

of lightning is also observed in FY-4 LMI and ISS LIS on the southern edge of Xinjiang, but the lightning distribution patterns are not the same, and there is no such lightning area in the ground-based ADTD observations.

In summary, the FY-4A LMI group, ADTD stroke group and ISS LIS group have similar spatial distribution in inland China. Influenced by the monsoon climate of China, with the rain belt moving northward, the lightning group also moves northward from south China and then retreats southward from April to August. Therefore, the FY-4A lightning data are an indicator for studies of precipitation and strong convection. In addition, for west China including the Tibet Plateau, the spatial distribution of the lightning group of FY-4A LMI is quite different from the other two observations.

3.2 *Comparison of spatial distribution of lightning flash*

Lightning flash can describe the whole process of lightning and has great application value. Therefore, this paper also analyzes FY-4A LMI flash data. Fig. 7 shows the spatial distribution of lightning flash of FY-4A LMI and ISS LIS in China. Fig. 7a, 7c, 7e, 7g and 7i are for

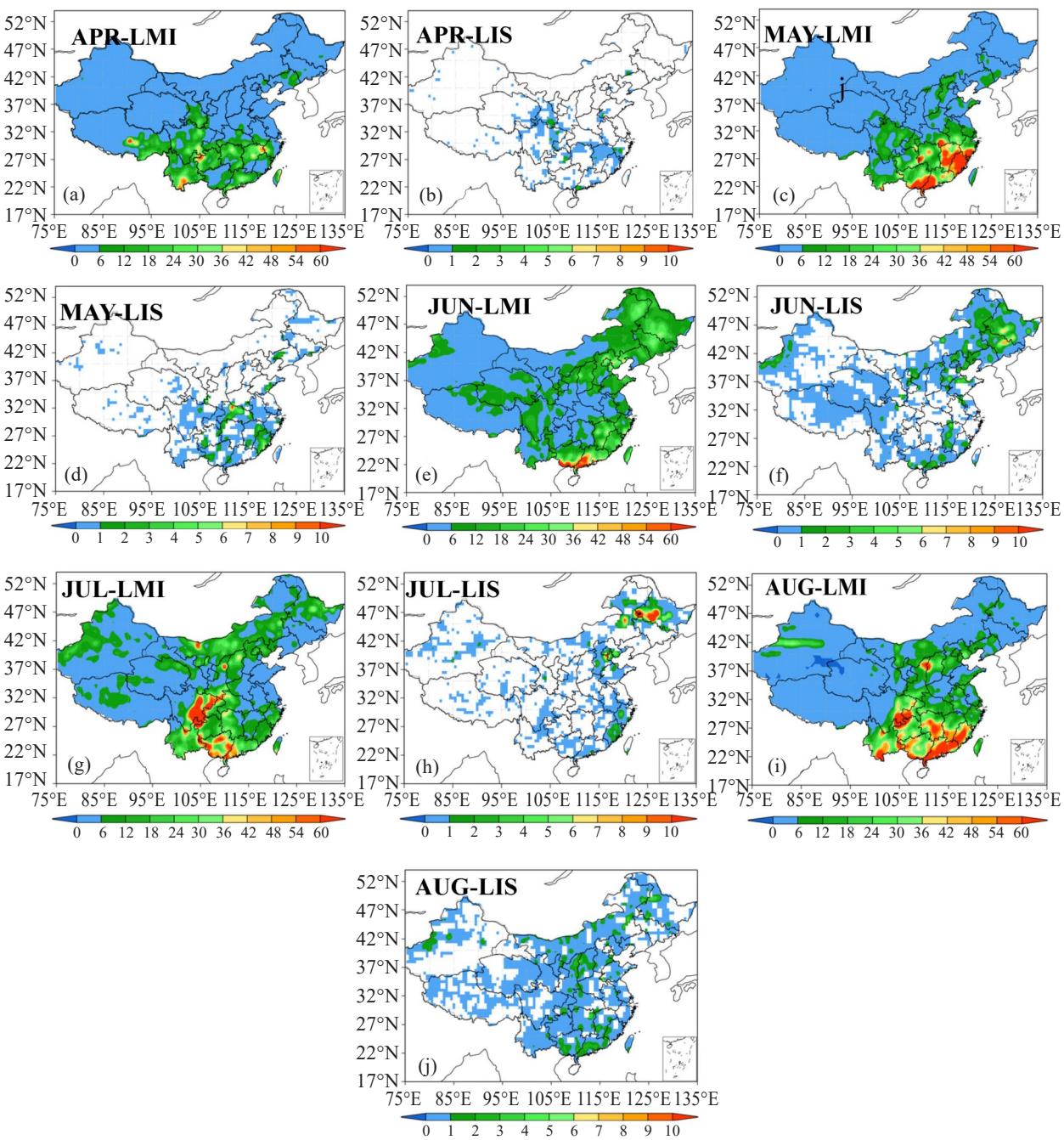

Figure 7. Spatial distribution of daily mean lightning flash frequency in inland China in 2018. (7a, 7c, 7e, 7g, and 7i) are the daily mean lightning flash spatial distributions of FY-4A from April to August; (7b, 7d, 7f, 7h, and 7j) are the daily mean lightning spatial distributions of ISS LIS lightning flash from April to August.

the FY-4A from April to August 2018, and Fig. 7b, 7d, 7f, 7h and 7i are for the ISS LIS. In general, the flash in April is mainly distributed in south China. From May to August, the flash gradually extends northward: in May, it extends to north China, and from June to July, it further extends to northeast China and central-eastern Inner Mongolia. In August, the flash of FY-4A and ISS LIS retreats. Both FY-4A and ISS LIS flash reflect this kind of distribution and movement trend and indicate the corresponding relationship between lightning flash and rain belt. Similar to the lightning group, the distribution of high-value flash area of FY-4A and ISS LIS is basically similar, and the frequency of FY-4A flash is higher than that of ISS LIS, which is related to the fact

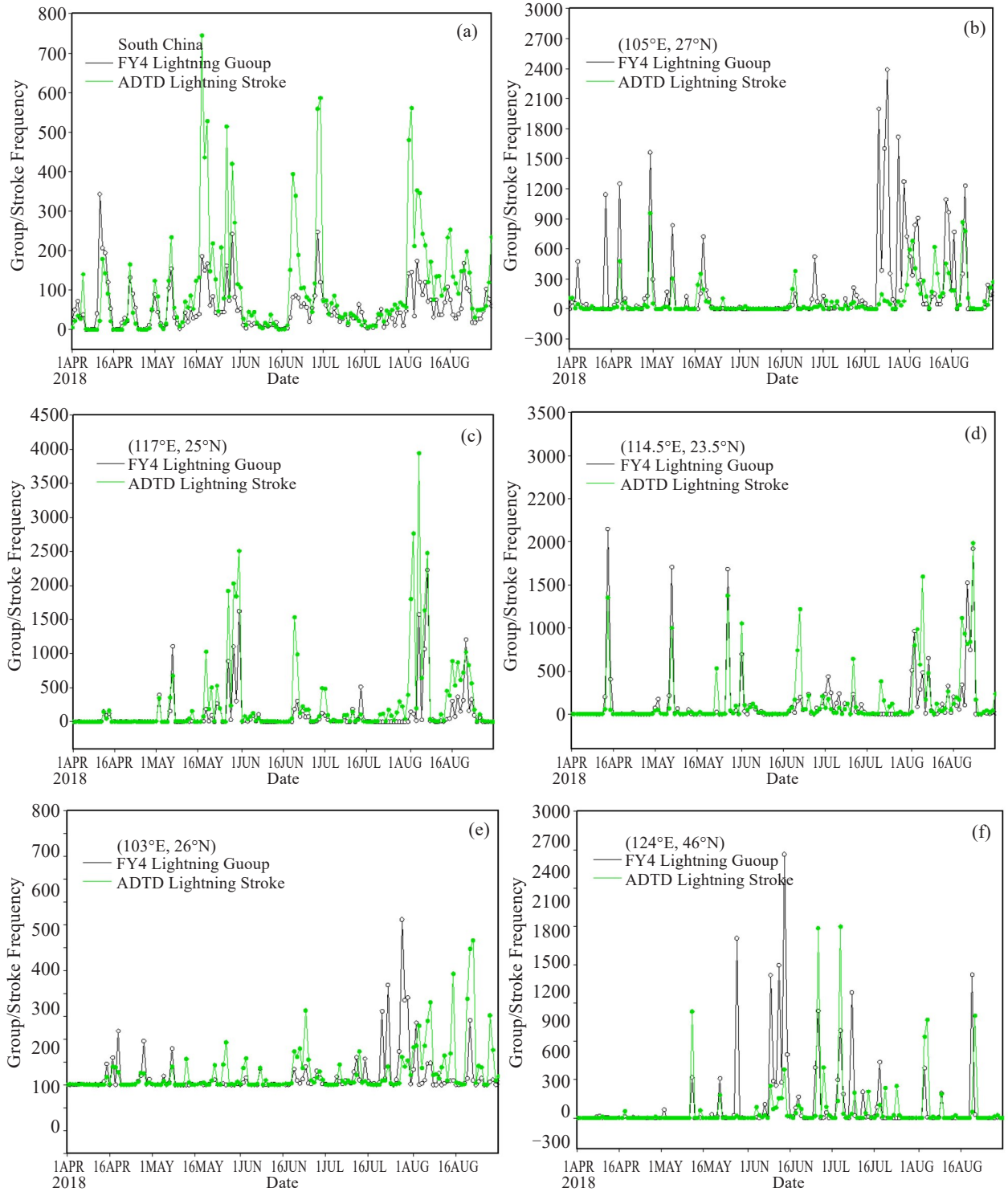

Figure 8. Time series of daily mean lightning frequency in southeast China and the five centers of high lightning occurrence in southeast China. The black line is the lightning frequency time series of the FY-4A group. The green line is the lightning frequency time series of the ground-based ADTD stroke. The five high-value centers are located at (105°E, 27°N), (117°E, 25°N), (114.5°E, 23.5°N), (103°E, 26°N), and (124°E, 46°N). (a) - (f) are the time series for southeast China and the five centers, respectively.

that FY-4A is a geostationary orbit satellite with higher frequency than ISS LIS does.

3.3 *Comparison of lightning temporal variation*

The spatial distribution of the lightning group and flash from April to August 2018 shows that southeast China is an area of high lightning occurrence and that there are several high-value centers. In this study, five lightning high-value centers are selected. For all of southeast China and each high-value center, the consistency of the daily variation trend of the lightning group frequency between FY-4A LMI and the ground-based ADTD stroke from 1 April to 31 August 2018 is analyzed. The range of southeast China is 22−35° N and 110−125° E. The five high-value centers are located at (105° E, 27° N), (117° E, 25° N), (114.5° E, 23.5° N), (103° E, 26° N), and (124° E, 46° N). The temporal variation in the daily mean lightning group frequency in southeast China is shown in Fig. 8a. Take five high-value centers as the center, obtain the average value within the range of 0.5° × 0.5° longitude and latitude from the center, and draw the daily average lightning frequency variation curve of five centers as shown in Fig. 8b~8f. The black line in Fig. 8 is the lightning group frequency observed by FY-4A LMI, and the green line is the lightning stroke frequency recorded by the ADTD ground-based observation. For the five centers and southeast China, the correspondence between high and low values of the FY-4A LMI group and ADTD stroke is basically similar. The temporal variation trend shows good consistency. From the perspective of the entire southeast region, the daily average value of ADTD stroke is higher than that of FY-4A LMI.

3.4 *Analysis of the spatial distribution of the FY-4A and ISS LIS lightning event data*

Because the ISS LIS follows a low-orbit path, its transit time over China is limited. The observation of any given fixed location occurs only once per day, whereas FY-4A observes the entire region of China every 2 ms. Hence, it can be assumed that when the ISS LIS observes lightning, FY-4A also detects lightning. Therefore, in this study, the ISS LIS event data are matched with the FY-4A event data point by point, and the spatial distribution of the matched samples is shown in Fig. 9. If both the ISS LIS and FY-4A detect lightning, the spot is marked with a red dot. If the ISS LIS detected lightning, while FY-4A did not, the spot is marked with a blue dot. The rule for spatiotemporal matching is a time difference that is less than 8.0 s and a spatial distance within 0.5° latitude and longitude.

Figure 9a~ 9e shows the spatial distribution of matching consistency from April to August, respectively. Overall, consistency is higher in April, May and July of 2018, and slightly lower in June and August. The detection consistency of south China is high. Inconsistency mainly occurs in northeast China and the Tibetan Plateau. There is also a small number of missed measurements in Xinjiang. In particular, from June to August, ISS LIS detected lightning in the interior of the plateau, and FY-4A LMI missed it. Overall, the FY-4A LMI data show relatively good consistency with similar satellite data, but there are discrepancies between the FY-4A and ISS LIS lightning observations in the Tibetan Plateau and northeast China.

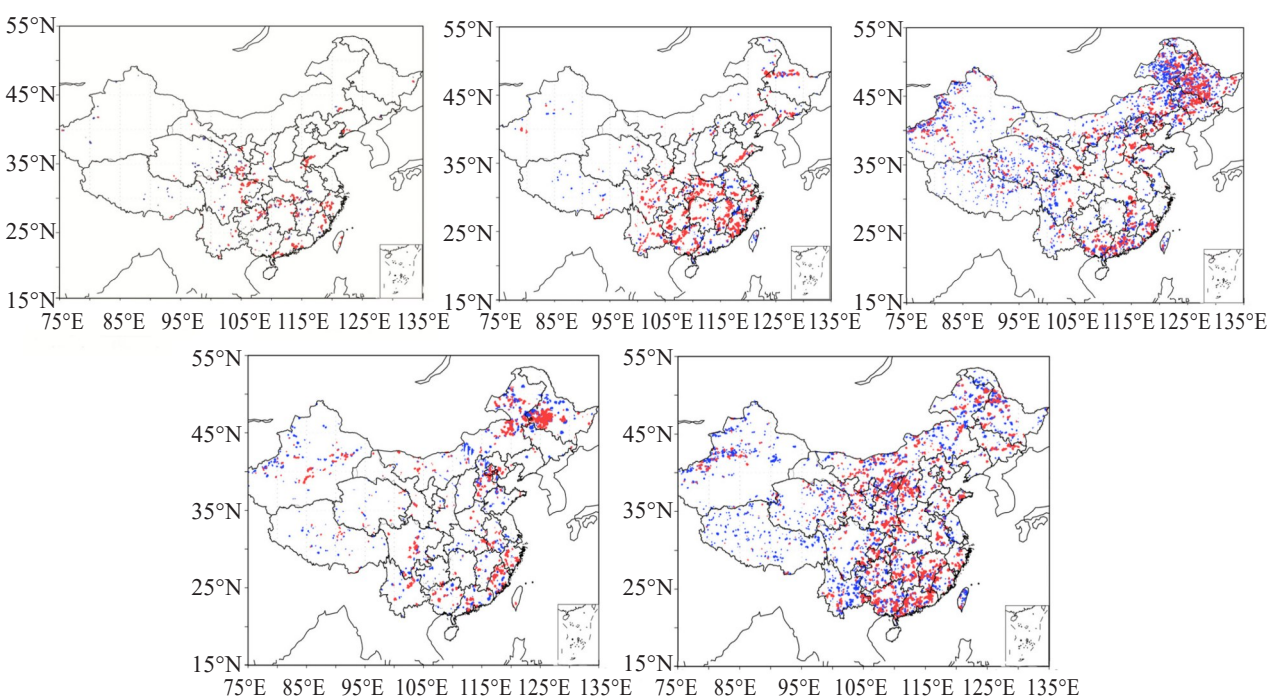

Figure 9. Spatial distribution of the point-by-point matching results of the ISS LIS and FY-4A. (a)-(e) correspond to the matching results in each month from April to August in 2018, respectively. Red dots: both the ISS LIS and FY-4A observed lightning; blue dots: the ISS LIS observed lightning, while FY-4A did not.

3.5 *Quantitative comparison of FY-4A LMI lightning event, group and flash*

We divide China into six regions to further quantify the consistency rate of lightning event, group and flash between FY-4A LMI and ISS LIS. The six regions, shown in Fig. 10, are divided mainly based on the spatial distribution of lightning occurrence frequency. The six regions are named according to their locations in China. Region A: south China. Region B: north China; Region C: southwest China; Region D: west China; Region E: northeast China; Region F: central Inner Mongolia.

Using the above algorithm to obtain the matching data sample database, the consistency rates of lightning for the six regions between FY-4A LMI and the ISS LIS are quantitatively calculated. The obtained statistical results and total sample numbers for event, group, and flash from April to August 2018 are shown in Table 1, Table 2 and Table 3, respectively.

As shown in Table 1, the consistency rate over the entire region of inland China between the FY-4A and ISS LIS lightning event observations is relatively high. The consistency rates from April to August are, in chronological order, 75.24%, 80.59%, 49.75%, 64.56%, and 52.02% from April to August. Except for that in June, the consistency rate between the two datasets is greater than 50%, and the consistency rates in April and May exceed 75.0%. In each month, the consistency rates of north China are from 48.69% to 97.51%, which are the relative high compared with those of the other regions. The consistency rates in south China and southwest China are also relatively high. Except for the slightly lower value of 48.27% in south China in June, the values in other months are all over 60%. The northeast region of China and central Inner Mongolia have relatively low consistency. West China has the worst consistency; the agreement rates in April and August are only 24.51% and 20.08%, respectively. The main part of the western region is the Tibetan Plateau. It can be seen that compared with that of ISS LIS, the FY-4A lightning event data show a relatively low detection rate of lightning over the Plateau. The in-orbit algorithm of the Real-Time Event Processor(RTEP) to extract events from the frame-to-frame raw data may mainly account for the FY-4A LMI's low lightning detection capability over the Plateau, which indicates that the algorithm requires a smaller threshold when filtering false signal and more sensitive background estimation over the Tibetan Plateau [33].

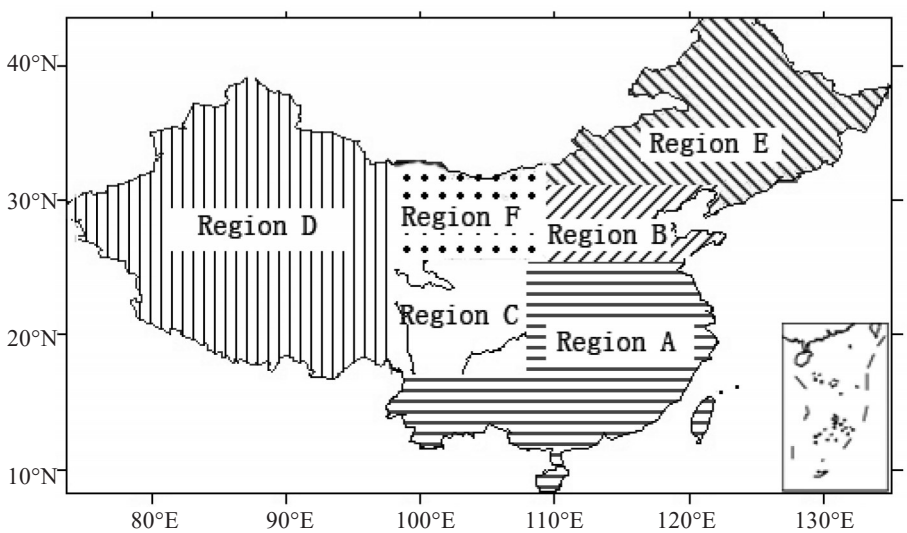

Figure 10. Distribution of six regions in China. Region A: south China; Region B: north China; Region C: southwest China; Region D: west China; Region E: northeast China; Region F: central Inner Mongolia.

Table 1. Statistical results of the consistency rates between the FY-4A and ISS LIS lightning event data from April to August 2018.

Month	April 2018		May 2018		June 2018		July 2018		August 2018	
	Consistency rate (%)	Sample number	Consistency rate (%)	Sample number	Consistency rate (%)	Sample number	Consistency rate (%)	Sample number	Consistency rate (%)	Sample number
China	75.24	46441	80.59	159431	49.75	287734	64.56	138325	52.02	266060
Region A	76.28	25391	82.97	118893	48.87	61963	67.81	33105	60.56	111202
Region B	97.51	3009	63.84	3484	48.69	31568	65.59	16426	67.23	26735
Region C	76.08	16341	89.46	22742	58.04	13585	5378	5008	53.72	29139
Region D	24.51	2071	52.75	5200	34.50	38560	43.88	14989	20.08	29853
Region E	55.10	1020	76.18	17612	53.69	128933	68.62	65555	44.98	54271
Region F	53.36	1535	52.10	1336	47.79	12689	63.00	3373	54.82	25140

As seen from Table 2, the lightning group consistency rate is significantly lower than the lightning event rate. The consistency rate of five months is lower than 50% except for that of June. The consistency rate of lightning flash (Table 3) is lower than 50% except for that of April too, and it is still slightly higher in south China.

Figure 11 shows the monthly distribution curve of the consistency rate of FY-4A LMI, ISS LIS event, group and flash in six regions of inland China.

From the time variation in inland China (Fig. 11a), the consistency rate of lightning events between FY-4A LMI and ISS LIS is 49.75% to 87.44%, which is lower in June and August. The consistency rate of group is approximately 50%, which is lower than that of event, and the consistency rate of flash is lower than that of group. It can be seen that in the process of calculating from lightning event to group and then to flash, both kinds of data introduce a calculation error, which makes the data quality decline. The other six regions show a trend in which the event consistency rate is better than that of group and flash (Fig. 11b~11g). It is worth noting that in the regions with dense lightning in south and north China, the consistency rate of group and flash of FY-4A lightning in July is poor, approximately 20%. In general, the consistency rate of FY-4A lightning and ISS

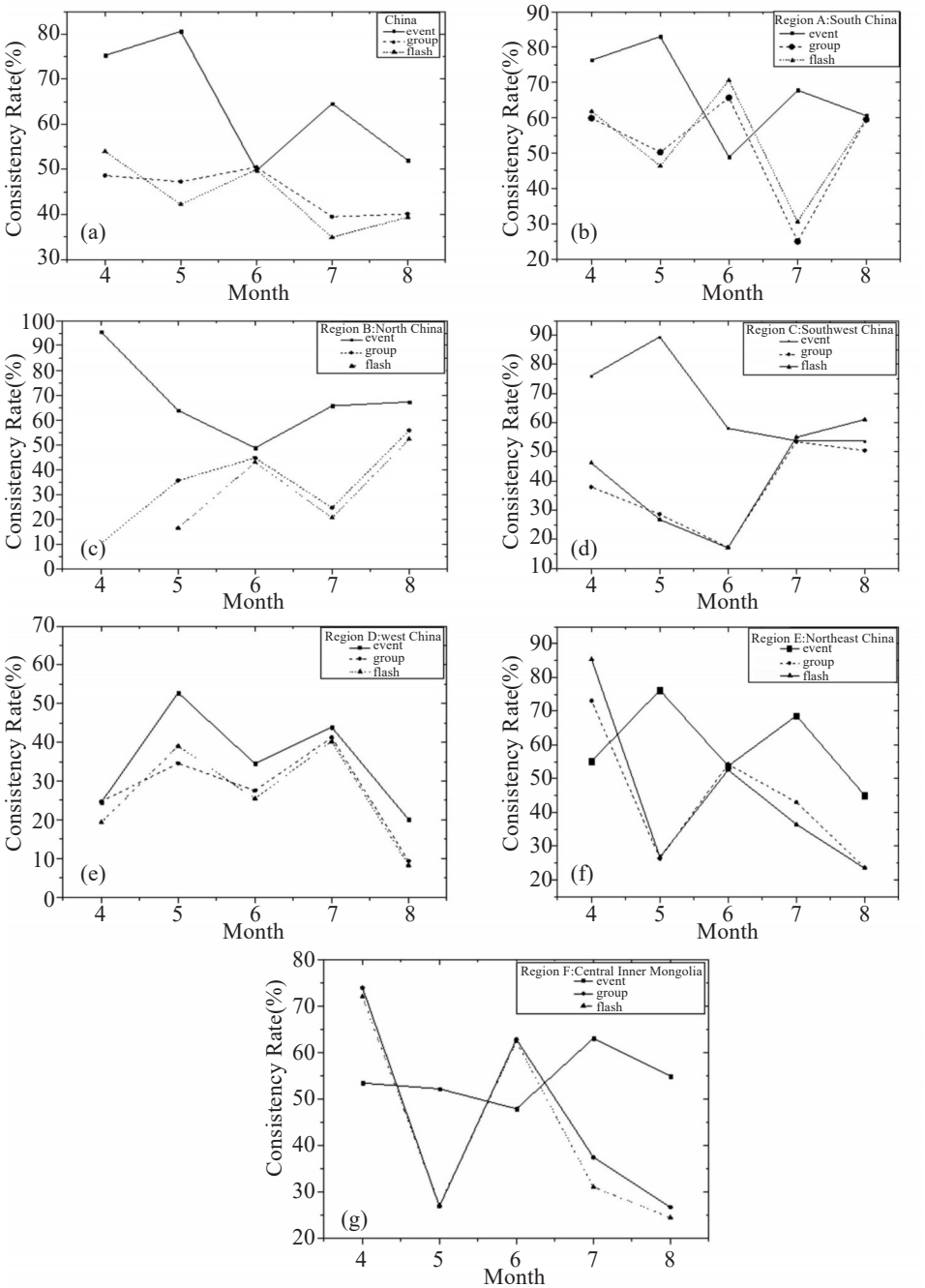

Figure 11. Monthly variation curve of the consistency rate of FY-4A LMI and ISS LIS in inland China and six regions. (a): Inland China; (b): Region A: south China; (c): Region B: north China; (d): Region C: southwest China; (e): Region D: west China; (f): Region E: northeast China; (g): Region F: central Inner Mongolia.

Table 2. Statistical results of the consistency rates between the FY-4A and ISS LIS lightning group data from April to August 2018.

Month	April 2018		May 2018		June 2018		July 2018		August 2018	
	Consistency rate (%)	Sample number	Consistency rate (%)	Sample number	Consistency rate (%)	Sample number	Consistency rate (%)	Sample number	Consistency rate (%)	Sample number
China	48.62	14787	47.26	43672	50.49	89676	39.49	47628	40.13	74420
Region A	59.88	7822	50.24	31675	65.66	15812	24.98	8314	59.45	27728
Region B	10.3	808	35.50	1166	44.67	10718	24.53	4715	55.75	7023
Region C	37.91	5288	28.55	6812	17.21	3672	53.48	1374	50.43	8220
Region D	24.68	636	34.54	1575	27.51	12139	41.22	4591	9.33	9523
Region E	73.05	449	26.29	4849	54.24	42826	42.96	27540	23.59	16914
Region F	73.86	528	26.78	392	62.76	4369	37.35	1138	26.61	7316

Table 3. Statistical results of the consistency rates between the FY-4A and ISS LIS lightning flash data from April to August 2018.

Month	April 2018		May 2018		June 2018		July 2018		August 2018	
	Consistency rate (%)	Sample number	Consistency rate (%)	Sample number	Consistency rate (%)	Sample number	Consistency rate (%)	Sample number	Consistency rate (%)	Sample number
China	53.96	1679	42.19	5715	49.73	13053	34.92	6911	39.36	10353
Region A	61.79	861	46.33	4111	70.61	2052	30.59	791	59.83	3505
Region B	——	0	16.35	214	42.81	1556	20.48	1074	52.19	1188
Region C	46.12	555	26.76	893	17.04	575	54.97	142	61.08	979
Region D	19.28	83	39.02	164	25.43	2013	40.22	469	8.20	1451
Region E	85.33	75	26.71	569	52.53	6110	36.41	4271	23.38	2370
Region F	71.91	89	27.03	37	62.29	740	30.95	168	24.34	1183

LIS monitoring is relatively low in west China, while in other regions it is relatively high, but there is no universal law for each month.

4 CONCLUSIONS AND DISCUSSION

The accuracy of the FY-4A lightning data is the basis for relevant scientific research. In this study, we assessed the accuracy of the FY-4A LMI lightning event, group, and flash data by a qualitative comparison of the lightning spatiotemporal distribution characteristics and a quantitative comparison of the spatiotemporal matching among the FY-4A LMI data, ground-based ADTD observation network data, and US ISS LIS lightning detection data. The results show the following:

(1) The spatial distribution of the FY-4A lightning group in China is consistent with that of the ground-based ADTD stroke and ISS LIS group. The observation of three kinds of data is consistent in south China, north China, central China, east China and southwest of the Plateau. In addition, the distribution of lightning extends from south to north China and then has a trend of retrogression from April to August, which is quite consistent with the moving characteristics of the rain belt affected by the monsoon climate in China. Therefore, the spatial distribution of FY-4A LMI lightning group data is reasonable, which also reflects that FY-4A LMI can capture the lightning occurrence in inland China. However, the frequency of ADTD stroke is higher than that of the FY-4A LMI group from May to August. It is possible that the number of lightning groups calculated by FY-4A is relatively lower in relation to the clustering algorithm of FY-4A LMI.

(2) The spatial distribution trend of FY-4A LMI flash and ISS LIS flash shows good consistency. The frequency of FY-4A lightning is much higher than that of ISS LIS, which is related to the orbit characteristics of the satellite carrying the lightning instrument. The consistent spatial distribution of the two flash datasets shows that FY-4A LMI flash data can reflect the distribution of the lightning process.

(3) The daily variation in FY-4A lightning group frequency is consistent with that of ADTD stroke from April to August.

(4) Quantitative statistics show that the consistency rate of FY-4A LMI and ISS LIS events is relatively high, but lower with group and flash.

(5) Compared with the data collected by the ISS LIS and the ground-based ADTD, FY-4A LMI observes fewer lightning events in the Tibetan Plateau.

The lightning detection data of the FY-4A satellite has many advantages such as high temporal resolution, high stability, and continuous observation compared with data collected by ground observation and low-orbit satellite observation. However, its detection principle is completely different from that of ground flash, and it cannot be treated as a real lightning strike, which requires attention in applications. In addition, the ground lightning data contains information such as lightning

intensity and steepness, but the satellite lightning only has location information. They can be used in combination and complement each other.

***Acknowledgments*:** We thank the NASA EOSDIS Global Hydrology Resource Center Distributed Active Archive Center for providing the ISS LIS dataset, and we thank the Meteorological Observation Center, China Meteorological Administration for providing ADTD lightning data.

REFERENCES

[1] PRICE C. Evidence for a link between global lightning activity and upper tropospheric water vapour [J]. Nature, 2000, 406(6793): 290-293, https://doi. org / 10.1038 / 35018543.

[2] BOND D W, STEIGER S, ZHANG R, et al. The importance of NO_x production by lightning in the tropics [J]. Atmos Environ, 2002, 36(9): 1509-1519, https://doi. org/10.1016/S1352-2310(01)00553-2.

[3] TOUMI R, HAIGH J D, LAW K S. A tropospheric ozone lightning climate feedback [J]. Geophys Res Lett, 1996, 23 (9): 1037-1040, https://doi.org/10.1029/96GL00944.

[4] WILLIAMS E R. The Schumann resonance: A Global thermometer [J]. Science, 1992, 256(5060): 1184-1187, https://doi.org/10.1126/science.256.5060.1184.

[5] WILLIAMS E R, RUTLEDGE A A, GEOTIS S G, et al. A radar and electrical study of tropical hot towers [J]. J Atmos Sci, 1992, 49(15): 1386-1395, https://doi. org / 10.1175/1520-0469(1992)049<1386:ARAESO>2.0.CO;2.

[6] GOODMAN S J, BUECHLER D E, KNUPP K, et al. The 1997-1998 El Niño event and related wintertime lightning variations in the Southeastern United States [J]. Geophys Res Lett, 2000, 27(4): 541-544, https://doi. org / 10.1029 / 1999GL010808.

[7] HAMID E F, KAWASAKI Z I, MARDIANA R. Impact of the 1997-98 El Niño event on lightning activity over Indonesia [J]. Geophys Res Lett, 2001, 28(1): 147-150, https://doi.org/10.1029/2000GL011374.

[8] BLAKESLEE R J, CHRISTIAN H J, STEWART M F. Lightning Imaging Sensor(LIS) for the international Space Station (ISS): Mission Description and Science Goals [C]// XV International Conference on Atmospheric Electricity. Oklahoma: 2014.

[9] LIU Rui-xia,LIU Jie, PESSI Antti, et al. Preliminary study on the influence of FY-4 lightning data assimilation on precipitation predictions [J]. J Trop Meteor, 2019, 25(4): 528-541, https://doi. org / 10.16555 / j. 1006-8775.2019.04.009.

[10] YANG Zhao-li, WAN Qi-lin, WU Dui, et al. The relationship between air chemical pollution and lightning activities in pearl river delta region [J]. J Trop Meteor , 2013, 29(6): 947-954 (in Chinese).

[11] WANG Yan-dong, ZHOU Yun-jun, WANG Xi-yang, et al. A study on the assimilation method of lightning data with mesoscale model WRF [J]. J Trop Meteor, 2014, 30(2): 281-292 (in Chinese).

[12] PESSI A, BUSINGER S. Relationships between lightning, precipitation, and hydrometeor characteristics over the North Pacific Ocean[J]. Meteor Appl, 2009, 48: 833-848.

[13] DONG Z , DAN Jian-Ru, ZHANG Yi-Jun, et al. Regional Differences of relationship between cloiud to ground lightning and precipitation in China [J]. J Trop Meteor, 2012, 28(4): 569-576(in Chinese).

[14] LI Zhao-Rong, FU Shuang-Xi, LI Bao-Zi , et al. Oberving study lightning characteristics on hail cloud [J]. J Trop Meteor, 2005, 12(1): 93-94.

[15] BIAGI C J, CUMMINS K L, KEHOE K E, et al. National lightning detection network (NLDN) performance in southern Arizona, Texas, and Oklahoma in 2003-2004 [J]. J Geophys Res: Atmos, 2007, 112(D5): D05208, https:// doi.org/10.1029/2006JD007341.

[16] CHRISTIAN H J, BLAKESLEE R J, GOODMAN S J. The detection of lightning from geostationary orbit [J]. J Geophys Res, 1989, 94(D11): 13329-13337, https://doi. org/10.1029/JD094iD11p13329.

[17] BOCCIPPIO D J, KOSHAK W J, BLAKESLEE R J. Performance assessment of the optical transient detector and lightning Imaging sensor, Part I: Predicted diurnal variability [J]. J Atmos Oceanic Technol, 2002, 19(9): 1318-1332, https://doi.org/10.1175/1520-0426(2002)019< 1318:PAOTOT>2.0.CO;2.

[18] CHRISTIAN H J, BLAKESLEE R J, BOCCIPPIO D J, et al. Global frequency and distribution of lightning as observed from space by the optical transient detector [J]. J Geophys Res, 2003, 108(D1): 4005, https://doi. org / 10.1029/2002JD002347.

[19] LIANG Hua, BAO Shu-long, CHENG Qiang, et al. Design and implementation of FY-4 geostationary lightning imager [J]. Aerospace Shanghai, 2017, 34(4): 43-51 (in Chinese).

[20] SCHULTZ C J, W A PETERSEN, L D CAREY. Preliminary development and evaluation of lightning jump algorithms for the real-time detection of severe weather [J]. J Appl Meteor Climatol, 2009, 48: 2543-2563, https://doi.org/10.1175/2009JAMC2237.1.

[21] GATLIN P N, GOODMAN S J. A total lightning trending algorithm to identify severe thunderstorms [J]. J Atmos Oceanic Technol, 2010, 27(1): 3-22, https://doi. org / 10.1175/2009JTECHA1286.1.

[22] STANO G T, SCHULTZ C J, CAREY L D, et al. Total lightning observations and tools for the 20 May 2013 Moore, Oklahoma, tornadic supercell [J]. J Oper Meteor, 2014, 2: 71-88, https://doi. org / 10.15191 / nwajom.2014.0207.

[23] GOODMAN S J, BLAKESLEE R J, WILLIAM J K, et al. The GOES-R geostationary lightning mapper (GLM) [J]. Atmos Res, 2013, 125-126: 34-49, https://doi. org / 10.1016/j.atmosres.2013.01.006.

[24] BAO Shu-long, TANG Shao-fan, LI Yun-fei, et al. Real-time detection technology of instantaneous point-source multi-target lighting signal on geostationary orbit [J]. Infrared and Laser Engineering, 2012, 41(9): 2390-2395 (in Chinese).

[25] YANG J, ZHANG Z, WEI C, et al. Introducing the new generation of Chinese geostationary weather satellite-FengYun 4(FY-4) [J]. Bull Amer Meteor Soc, 2017, 98 (8): 1637-1659, https://doi. org / 10.1175 / BAMS-D-16-0065.1.

[26] CAO Dong-jie. The development of product algorithm of the Fengyun-4 geostationary lightning mapping imager [J]. Adv Meteorol Sci Technol, 2016, 6(1): 94-98 (in Chinese).

[27] LI Jing-xiao, GUO Feng-xia, HU Hai-bo, et al.

Comparative analysis of SAFIR and ADTD lightning location data over Beijing and its circumjacent regions [J]. Plateau Meteorology, 2017, 36(4): 1115-1126 (in Chinese), https://doi. org / 10.7522 / j. issn. 1000-0534.2016.00132.

[28] XIA Ru-di, ZHANG Da-Lin, WANG Bai-lin. A 6-yr cloud-to-ground lightning climatology and its relationship to rainfall over central and eastern China [J]. J Appl Meteorol Climatol, 2015, 54(12): 2443-2460, https://doi. org/10.1175/JAMC-D-15-0029.1.

[29] MENG Qing, ZHAO Jun-zhuang, ZHANG Yi-jun, et al. Lightning Detection and Location System, Part 1 Technical Specification. Profession Standard of the People's Republic Of China (QX / T79 - 2007) (in Chinese), 2007.

[30] BLAKESLEE R, MACH D M, STEWART M F, et al. NRT Lightning Imaging Sensor (LIS) on International Space Station (ISS) Provisional Science Data [indicate subset used]. Dataset available online from the NASA EOSDIS Global Hydrology Resource Center Distributed Active Archive Center, Huntsville, Alabama, U. S. A. 2017. doi:10.5067/LIS/ISSLIS/ DATA205

[31] BLAKESLEE R, CHRISTIAN H J, MACH D M, et al. Lightning Imaging Sensor on the International Space Station: Assessments and Results from First Year Operations [C]// Paper presented at the XVI International Conference on Atmospheric Electricity, Nara city, Nara, Japan, 2018, June 17 -22.

[32] BLAKESLEE R, KOSHAK W. LIS on ISS: Expanded Global Coverage and Enhanced Applications [Z]. The Earth Observer, 2016, 28 (3): 4-14. https://eospso. gsfc. nasa.gov/earthobserver/mayjun-2016.

[33] WEN Hui, HUANG Fu-xiang, LIU Rui-xia, et al. Characteristics of lightning signals over the Tibetan Plateau and the capability of FY-4A LMI lightning detection in the Plateau [J]. International J Remote Sensing, 2020, 41(12): 4603-4623, https://doi. org / 10.1080/01431161.2020.1723176

[34] SCOTT D R, DUSTIN T S. Evaluating WWLLN performance relative to TRMM / LIS [J]. Geophys Res Lett, 2013, 40(10): 2344-2348, https://doi. org / 10.1002 / grl.50428.

[35] ZHU Jie. Comparison of the satellite-based Lightning Imaging Sensor (LIS) against the ground-based national lightning monitoring network [J]. Progress in Geophys, 2018, 33(2): 541-546 (in Chinese), https://doi. org / 10.6038/pg2018AA0631.

Citation: LIU Rui-xia, LU Qi-feng, CHEN Min, et al. Quality assessment of FY-4A lightning data in inland China [J]. J Trop Meteor, 2020, 26(3): 286-299, https://doi.org/10.46267/j.1006-8775.2020.026.